Oriented chlorine atoms as a probe of the nonadiabatic photodissociation dynamics of molecular chlorine

Andrew J. Alexander,[a] Zee Hwan Kim, S. Alex Kandel,[b] and Richard N. Zare[c]
Department of Chemistry, Stanford University, Stanford, California 94305

T. Peter Rakitzis
Institute of Electronic Structure and Laser, Foundation for Research and Technology—Hellas, 711 10 Heraklion—Crete, Greece

Yukako Asano and Satoshi Yabushita
Department of Chemistry, Faculty of Science and Technology, Keio University, 3-14-1 Hiyoshi, Kohoku-ku, Yokohama 223-8522, Japan

(Received 27 June 2000; accepted 1 September 2000)

Molecular chlorine was photolyzed using circularly polarized radiation at 310 and 330 nm, and orientation moments of the chlorine-atom $Cl(^2P_j)$ photofragment distributions were measured by resonance enhanced multiphoton ionization using circularly polarized light with Doppler resolution. The product atoms were found to be strongly oriented in the laboratory as a result of both incoherent and coherent dissociation mechanisms, and the orientation moments contributed by each of these mechanisms have been separately measured. The experimental results can be explained by nonadiabatic transitions from the $C\,^1\Pi_{1u}$ state to higher states of $\Omega=1_u$ symmetry, induced by radial derivative coupling. *Ab initio* calculations indicate strong Rosen–Zener–Demkov noncrossing-type radial derivative couplings between states of 1_u symmetry. The observed angular distribution (β parameter) indicates that 88% of $Cl^*(^2P_{1/2})$ fragments produced at 310 nm originate from a perpendicular transition to the *C* state. The orientation measurements suggest that $67\pm16\%$ of $^{35}Cl^*(^2P_{1/2})$ atoms dissociate via the $1_u(^3\Sigma^+_{1u})$ state, and $21\pm6\%$ dissociate via the $1_u(^3\Delta_{1u})$ state. © *2000 American Institute of Physics.* [S0021-9606(00)01444-6]

I. INTRODUCTION

The electronic states of chlorine molecules that are accessed by ultraviolet radiation in the region around 330 nm have been of great importance to our understanding of molecular bonding and the dynamics that occur when molecules dissociate.[1] Indeed, the halogen molecules in general have provided a standard for theoretical and experimental studies of the electronic states and potential energy curves of diatomic molecules.[2] The ultraviolet absorption spectrum of Cl_2 is continuous between 250 and 450 nm, with a maximum at ~330 nm. Experimental measurements of the fine-structure branching ratios following dissociation caused by ultraviolet radiation have been made by a number of groups.[3] Samartzis *et al.*[4,5] have made detailed ion-imaging and velocity-map imaging studies of Cl_2 photodissociation, and have reported angular distributions (parametrized by the second-order Legendre moment of the distribution, β), and branching ratios. Present understanding has it that the dissociation around 330 nm is dominated by a perpendicular transition to the $C\,^1\Pi_{1u}$ state, with increasing contributions from the $B\,^3\Pi^+_{0u}$ state at longer wavelengths, although the question of involvement of the $A\,^3\Pi_{1u}$ state has remained open.[3] Measurements of the chlorine atom photofragment alignment by Rakitzis *et al.*[6] and Bracker *et al.*[7] are consistent with the dissociation proceeding mainly by adiabatic dissociation via the *C* state, but have suggested that nonadiabatic transitions involving the *A* state do occur. The observation of a coherent alignment moment provides further support for the importance of homogeneous nonadiabatic transitions between the *C* and *A* states.[7]

To understand the involvement of states that correlate to produce $Cl^*(^2P_{1/2})$, Samartzis *et al.*[5] used their measurements of Cl* angular distributions, and Cl/Cl* branching ratios to estimate the degree of nonadiabatic transition from the *C* state to states that correlate to produce Cl+Cl*. Kim *et al.*[8] have reported measurements of the orientation of Cl* atoms as a function of photolysis energy. The coherent orientation moment $\mathrm{Im}[\mathbf{a}_1^{(1)}(\parallel,\perp)]$ can be related to the interference between dissociating pathways originating from parallel ($\parallel$) and perpendicular ($\perp$) transitions whose final states correlate to the same asymptotic limit, in this case Cl+Cl*.[8–10] These measurements, along with high-level *ab initio* calculations by Yabushita,[11,12] have challenged us to make a more detailed investigation of the nonadiabatic transitions, the states involved, and the dynamics of the dissociation process.

In 1968, van Brunt and Zare[13] predicted that the photodissociation of a diatomic molecule could produce polarized atomic fragments. Experimental observations of polarized

[a]Present address: Department of Chemistry, University of Edinburgh, West Mains Road, Edinburgh, EH9 3JJ, UK.
[b]Present address: Davey Laboratory, Pennsylvania State University, University Park, PA 16802.
[c]Author to whom correspondence should be addressed; electronic mail: zare@Stanford.EDU

 © 2000 American Institute of Physics

Downloaded 24 Feb 2012 to 171.64.124.19. Redistribution subject to AIP license or copyright; see http://jcp.aip.org/about/rights_and_permissions

atomic fragments were first made in the early 1980s by Vasyutinskii[14,15] and by Rothe *et al.*,[16] Vasyutinskii,[15,17] Siebbeles *et al.*,[9] and Mo *et al.*[18] have presented quantum mechanical treatments of atomic photofragment polarization. Recently, measurements of the polarization of the electronic angular momentum of photofragments have shown considerable promise for revealing details of the unbound states of molecules.[19–21] Although these studies cannot match the depth of information revealed by conventional spectroscopy, it is clear that they allow us to probe dynamics that were hitherto inaccessible.

Photofragment orientation can occur by coherent dissociation mechanisms, but can also be induced by using circularly polarized photolysis radiation; in this case, the directional nature of the photon angular momentum must be conserved in the laboratory frame. Zare and co-workers[22,23] have studied the orientation of CN fragments produced by dissociation of ICN using circularly polarized radiation. Vasyutinskii and co-workers[24–27] have made important theoretical and experimental studies using the optical magnetic birefringence (Faraday) technique. Recently, Korovin *et al.*[28] reported the first observation of spin-oriented Rb-atom photofragments, produced by photolysis of RbI at 266 nm using circularly polarized light. Their results indicated the presence of both coherent and incoherent dissociation mechanisms, although these mechanisms could not be quantified separately.

In this paper, we report the observation of electronically oriented Cl-atom photofragments from the dissociation of Cl_2 at 310 and 330 nm using circularly polarized photolysis and probe radiation. Our measurements support the presence of both coherent and incoherent dissociation mechanisms. From our measurements we estimate the extent of nonadiabatic radial derivative coupling that leads to production of Cl*, and we are able to identify the states that are involved in the nonadiabatic dynamics. In what follows we present a brief introduction to the experimental and theoretical methods employed (Sec. II). Results are presented in Sec. III and a discussion in Sec. IV. A brief summary and conclusions appear in Sec. V.

II. METHOD

A. Experiment

Full descriptions of the experimental apparatus and techniques used have been given elsewhere,[6,29] and only details pertinent to the present study will be given here. A dilute solution (~8%) of molecular chlorine (Matheson, 99.999%) in high-purity helium (Liquid Carbonic, 99.995%) was premixed and expanded into high vacuum through a pulsed nozzle (General Valve, Series 9, 0.6 mm orifice). The stagnation pressure of the sample used was typically 450 Torr. Chlorine was dissociated using circularly polarized light at 310 and 330 nm. A zero-order 308 nm quarter waveplate (CVI Laser) was used to control the circular polarization at 310 nm, and a Soleil-Babinet compensator (Special Optics Inc.) was used at 330 nm. Product chlorine atoms in the ground $Cl(^2P_{3/2})$ and excited $Cl^*(^2P_{1/2})$ states were detected selectively using 2+1 REMPI (resonance enhanced multiphoton ionization) at around 235 nm. The transitions used were $3s^23p^44p^2P^\circ_{1/2}-3s^23p^{5\,2}P^\circ_{3/2}$ at 236.518 nm and $3s^23p^44p\,^2P^\circ_{3/2}-3s^23p^{5\,2}P^\circ_{1/2}$ at 234.620 nm. These transitions were specifically chosen to be sensitive to the orientation moments of the electron angular momentum distribution. The atoms were probed using alternately left and right circularly polarized light on a shot-to-shot basis. Thin-film polarizers (CVI Laser) were used to improve the quality of the linearly polarized ultraviolet radiation. The circular polarization of the probe laser radiation was introduced by using a 241 nm zero-order quarter waveplate (CVI Laser) and the handedness was changed on a shot-to-shot basis using a photoelastic modulator (Hinds PEM-80). The high quality (>100:1) of probe laser circular polarization was confirmed by REMPI using the $Cl^*(3s^23p^44p;^2P^\circ_{1/2}-3s^23p^{5\,2}P^\circ_{1/2})$ transition at 237.074 nm.

The probe laser was arranged in a collinear counterpropagating geometry with respect to the photolysis laser. The dissociation and detection was carried out at the extraction region of a time-of-flight mass spectrometer. Unlike previous studies, however, the total Cl^+ ion signal was collected, and the sensitivity to product velocity was achieved by scanning over the Doppler-broadened line shape of the REMPI transition. Because the chlorine atoms are traveling relatively fast ($\sim 2\ \mathrm{km\,s^{-1}}$) with a well-defined speed, no efforts were made to further narrow the linewidth of the probe dye laser (Spectra-Physics PDL-3; nominal fundamental linewidth $\sim 0.07\ \mathrm{cm^{-1}}$).

The definition of the handedness of circular polarization that we use is the conventional one, i.e., left circular polarization (LCP) has positive handedness or helicity, and obeys the right-hand rule with the thumb pointing in the direction of the propagation vector.[30] For LCP the electromagnetic field rotates counterclockwise in a fixed plane as viewed looking into the oncoming wave, and each photon has a projection of one unit of angular momentum ($+\hbar$) with respect to its propagation vector.[31] The absolute handedness of the circularly polarized light was determined using a single fused-silica Fresnel rhomb (CVI Laser). The absolute phase of the output of the rhomb can be calculated using Fresnel's equations.[30] The Fresnel rhomb was oriented in the beam path after the unknown circularly polarizing element; the $\pi/4$ phase of the two circularly polarizing elements either cancel or add to give linearly polarized light with 0 or $\pi/2$ phase. For example, if the light is initially horizontally polarized (HP), and after the two circular elements the light is also HP, we know that the two circular elements have the same handedness. Further, if we know that the Fresnel rhomb is physically oriented to give LCP, then the other circular element must also be set to give LCP.

B. Data analysis

For these experiments, the laboratory axis with highest symmetry (Z axis) is defined by the propagation vector of the circularly polarized (CP) photolysis radiation. We refer to Doppler profiles taken with CP probe radiation as D_L and D_R for the counterpropagating probe laser light being LCP or RCP, respectively. Isotropic profiles that do not depend on

Downloaded 24 Feb 2012 to 171.64.124.19. Redistribution subject to AIP license or copyright; see http://jcp.aip.org/about/rights_and_permissions

the orientation of the product atom can be defined as $D_{\mathrm{iso}} = D_L + D_R$. The corresponding anisotropic difference profiles that contain odd moment orientation information are defined as $D_{\mathrm{aniso}} = D_L - D_R$.

The laboratory frame detection probability in the present experiment can be conveniently written in terms of the $\mathbf{a}_q^{(k)}(p)$ moments of Rakitzis and Zare, where p is used to denote parallel ($\parallel$) or perpendicular ($\perp$) or mixed ($\parallel,\perp$) transitions:[10]

$$D_{\mathrm{lab}} = 1 + \beta P_2(\cos\Gamma) P_2(\cos\gamma) + G^1 s_1 \cos\Gamma \times \left[(1+\beta)\mathbf{a}_0^{(1)}(\perp)\cos^2\gamma - \frac{1}{\sqrt{2}}\mathrm{Re}[\mathbf{a}_1^{(1)}(\parallel,\perp)]\sin^2\gamma \right] + G^3 s_3 \cos\Gamma[(1+\beta)\mathbf{a}_0^{(3)}(\perp)\cos\gamma P_3(\cos\gamma) - \mathrm{Re}[\mathbf{a}_1^{(3)}(\parallel,\perp)]\sin^2\gamma(1-5\cos^2\gamma)]. \quad (1)$$

In Eq. (1) Γ is the angle of the CP probe propagation vector with respect to the CP photolysis propagation vector (the lab Z axis): In the present experiments $\Gamma = 180°$. γ is the angle between the direction of recoil of the fragments and the lab Z axis, and P_k denotes a Legendre polynomial of order k. For Cl* atoms, $j = 1/2$, and there are no moments with $k > 1$, i.e., the $\mathbf{a}_q^{(3)}(p)$ terms cannot exist. The sensitivity parameters for the REMPI process (s_k) can be easily calculated using the method of Mo and Suzuki:[32] In the notation of Rakitzis *et al.*[33] we find for ground-state Cl, $s_1 = -2.323$, $s_3 = -1.936$, and for excited-state Cl* we find $s_1 = -1.732$. We must also account for hyperfine depolarization of the product atoms,[34] for which we take the long-time limit of the nuclear hyperfine depolarization ratio: $G^1 = 0.5$, $G^3 = 0.2$ (Cl) and $G^1 = 0.375$ (Cl*).

As in previous works,[6,35] isotropic and anisotropic Doppler profiles were fitted with basis functions generated by a Monte Carlo simulation using Eq. (1). The translational anisotropy β parameter was taken from the work of Samartzis *et al.*,[5] and multiplied by -0.5 to account for the use of CP photolysis light.[36] The basis functions were convoluted with an empirical blurring function (Gaussian) to account for the laser linewidth. Figure 1 presents typical anisotropic basis functions for the $\mathbf{a}_0^{(1)}(\perp)$, $\mathrm{Re}[\mathbf{a}_1^{(1)}(\parallel,\perp)]$, and $\mathbf{a}_0^{(3)}(\perp)$. The Doppler forms of the $\mathbf{a}_0^{(1)}(\perp)$ and $\mathrm{Re}[\mathbf{a}_1^{(1)}(\parallel,\perp)]$ are clearly different, with the $\mathbf{a}_0^{(1)}(\perp)$ peaking for those fragments traveling toward and away from the probe laser light, and the $\mathrm{Re}[\mathbf{a}_1^{(1)}(\parallel,\perp)]$ showing a single peak for products at the line center. The $\mathbf{a}_0^{(3)}(\perp)$, on the other hand, shows oscillations, resulting from the third-order Legendre function in Eq. (1).

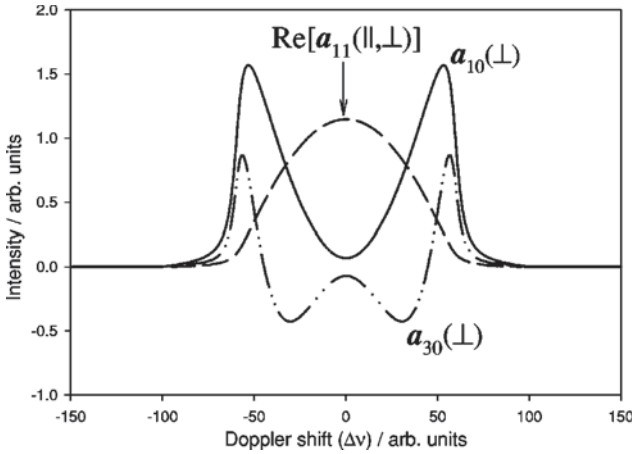

FIG. 1. Typical anisotropic Doppler profile basis functions for the moments $\mathbf{a}_0^{(1)}(\perp)$ (solid line) showing a double velocity peak, $\mathrm{Re}[\mathbf{a}_1^{(1)}(\parallel,\perp)]$ (dashed line) showing a single velocity peak, and $\mathbf{a}_0^{(3)}(\perp)$ (dot-dashed line) showing oscillations. All profiles have been broadened with an arbitrary Gaussian function to simulate the finite linewidth of the transition. The abscissa is scaled in arbitrary units of Doppler-shifted frequency and the moments have been scaled to show the most detail.

III. RESULTS

Figure 2 shows isotropic and anisotropic Doppler profiles for Cl and Cl* atoms from chlorine molecules photolyzed at 310 nm. Also shown are the fits obtained using the basis function method described previously. Both the Cl and Cl* data can be fitted using only the first-order orientation moment $\mathbf{a}_0^{(1)}(\perp)$: For the Cl atoms, we did not fit for contributions from $\mathbf{a}_0^{(3)}(\perp)$ because its presence cannot be detected within the limits of the experimental noise. Further, there appears to be no $\mathrm{Re}[\mathbf{a}_1^{(1)}(\parallel,\perp)]$ or $\mathrm{Re}[\mathbf{a}_1^{(3)}(\parallel,\perp)]$ in accordance with the Cl atoms being produced almost entirely by dissociation via a pure perpendicular transition to the C state.[5] In previous work, we have reported that the Cl* atoms display an $\mathrm{Im}[\mathbf{a}_1^{(1)}(\parallel,\perp)]$ at 310 nm, resulting from coherent dissociation via the B and C states.[8] However, at this wavelength we see no evidence of a $\mathrm{Re}[\mathbf{a}_1^{(1)}(\parallel,\perp)]$: The $\mathrm{Im}[\mathbf{a}_1^{(1)}(\parallel,\perp)]$ is dependent on the sine of the phase difference of radial wave functions created on the two curves, $\sin(\Delta\phi)$, whereas the $\mathrm{Re}[\mathbf{a}_1^{(1)}(\parallel,\perp)]$ has a $\cos(\Delta\phi)$ dependence.[9] Our previous measurements indicate that $\mathrm{Im}[\mathbf{a}_1^{(1)}(\parallel,\perp)]$ is large at 310 nm, and so we may expect the $\mathrm{Re}[\mathbf{a}_1^{(1)}(\parallel,\perp)]$ to be small, in agreement with the present results (see Sec. IV).

Figure 3 shows Doppler profiles with fits for Cl and Cl* atoms produced from chlorine molecules photolyzed at 330 nm. The Cl atom results do not show the two peaks of the $\mathbf{a}_0^{(1)}(\perp)$ so clearly, due to the slow speed of the Cl atoms and the frequency bandwidth of the laser. As was found at 310 nm, the Cl atoms are formed mainly via the C state, and we do not expect to see any $\mathrm{Re}[\mathbf{a}_1^{(1)}(\parallel,\perp)]$. The Cl* results at 330 nm, however, clearly show contributions from both $\mathbf{a}_0^{(1)}(\perp)$ and $\mathrm{Re}[\mathbf{a}_1^{(1)}(\parallel,\perp)]$, indicating the presence of both parallel and perpendicular transitions. We found that it was not possible to fit the Cl* data properly by assuming only an $\mathbf{a}_0^{(1)}(\perp)$ or only a $\mathrm{Re}[\mathbf{a}_1^{(1)}(\parallel,\perp)]$.

By integrating Eq. (1) with respect to $\cos\gamma$, we can write

$$\frac{I_L - I_R}{I_L + I_R} = \tfrac{1}{3} G^1 s_1 [(1+\beta)\mathbf{a}_0^{(1)}(\perp) - \sqrt{2}\mathbf{a}_1^{(1)}(\parallel,\perp)], \quad (2)$$

where $I_{L/R}$ is the ionization signal integrated over the Doppler line shape. Note that the $\mathbf{a}_0^{(3)}(\perp)$ term vanishes in the integration. Assuming that only $\mathbf{a}_0^{(1)}(\perp)$ needs to be considered, it is possible to obtain an estimate for this moment by taking the ratio of integrated difference to the integrated sum of the experimental data, which avoids the need to use the

Downloaded 24 Feb 2012 to 171.64.124.19. Redistribution subject to AIP license or copyright; see http://jcp.aip.org/about/rights_and_permissions

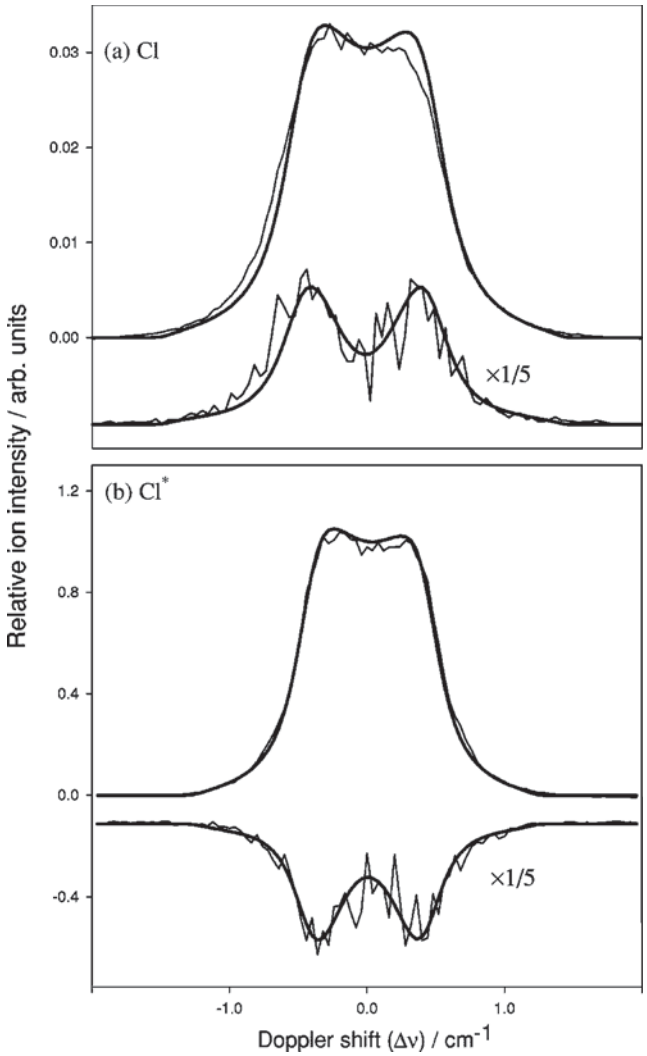

FIG. 2. Isotropic (upper trace) and anisotropic (lower trace) Doppler profiles for (a) $^{35}Cl(^2P_{3/2})$ atoms and (b) $^{35}Cl^*(^2P_{1/2})$ atoms at 310 nm. The isotropic Doppler profiles are not dependent on product orientation. The anisotropic profiles can be related to orientation moments of the electronic angular momentum distribution, as detailed in the text. Thin solid lines represent the experimental data, and thick solid lines are the fits obtained as detailed in the text.

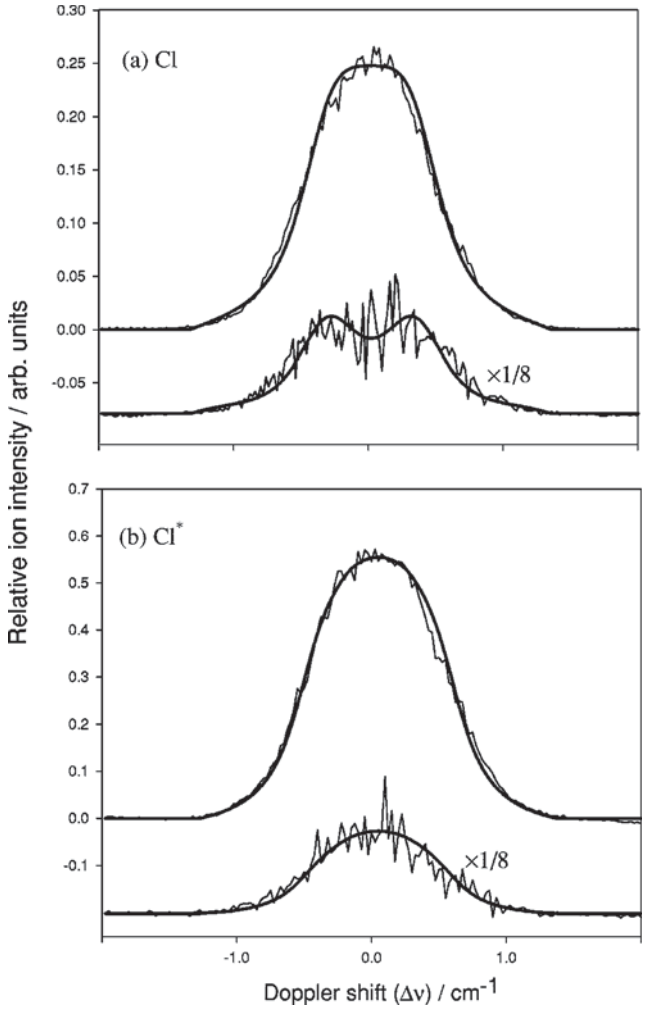

FIG. 3. As in Fig. 2 but showing data obtained at the photolysis wavelength of 330 nm.

basis fitting method. The results of this method, and of the basis function fitting are shown in Table I. For completeness, the integrated result for Cl* produced at 330 nm is also shown in Table I, although we cannot separate the $\mathbf{a}_0^{(1)}(\perp)$ and $\mathrm{Re}[\mathbf{a}_1^{(1)}(\parallel,\perp)]$ moments. The results for ^{35}Cl and ^{37}Cl are in excellent agreement, serving as independent measurements of the orientation. Contributions from an $\mathbf{a}_0^{(3)}(\perp)$ would modify the fitted $\mathbf{a}_0^{(1)}(\perp)$ value compared to the integrated value; however, the good agreement between the two analysis methods suggests that the $\mathbf{a}_0^{(3)}(\perp)$ contribution is small. The error bars for the integrated results were obtained from standard deviations across a set (typically 10) of measured profiles. The uncertainties listed for the fitting method that uses basis functions were obtained by a Monte Carlo sampling method that was applied to the averaged data; sampled fits that lay visibly beyond the random noise were discarded. The uncertainties obtained in this way appear smaller than the profile-to-profile variance, and we therefore feel that they do not represent true uncertainties for the measurement. The Monte Carlo method, however, does allow us to estimate the relative uncertainties in the $\mathbf{a}_0^{(1)}(\perp)$ and $\mathrm{Re}[\mathbf{a}_1^{(1)}(\parallel,\perp)]$ that contribute to the Cl* (330 nm) data: the covariance between these fitted moments is also reflected in the Monte Carlo uncertainties.

Possible sources of systematic error in our measurements include background signal from the probe laser, which would contribute to the isotropic but not to the anisotropic signal and tend to decrease the observed $\mathbf{a}_0^{(1)}(\perp)$: We estimate this effect to be less than 2% for the results in Table I. We used the β parameter taken from previous studies[3,5] to analyze our data, although we did not take account of uncertainties in those values. We estimate a possible additional 5% uncertainty resulting from uncertainties in the β parameter. Indeed, in a previous work[37] we have proposed the use of polarization moments as a more sensitive measurement of the β parameter.

A high quality of the CP light in these experiments was found to be crucial: We have observed that refractive elements (lenses, windows, etc.) can decrease the quality of polarization. The Soleil–Babinet compensator is calibrated for the wavelength being used, and we have found that it is

Downloaded 24 Feb 2012 to 171.64.124.19. Redistribution subject to AIP license or copyright; see http://jcp.aip.org/about/rights_and_permissions

TABLE I. Photofragment orientation moments obtained by fitting of Doppler profiles, and by integration (see the text for details) measured from the photolysis of Cl_2 at 310 and 330 nm. The integrated result for Cl* at 330 nm has been included for completeness. The translation anisotropies (β) used for the data analysis were taken from Samartzis *et al.* (Ref. 5), and have been multiplied by $-1/2$ to account for the use of circularly polarized photolysis light.

Photolysis wavelength/nm	Product atom	β	Fitted $\mathbf{a}_0^{(1)}(\perp)$	Integrated $\mathbf{a}_0^{(1)}(\perp)$
310	^{35}Cl	0.5	0.13±0.02	0.14±0.04
	^{37}Cl	0.5	0.18±0.02	0.20±0.04
	^{35}Cl*	0.32	−0.24±0.01	−0.27±0.06
	^{37}Cl*	0.32	−0.23±0.02	−0.30±0.07
330	^{35}Cl	0.5	0.23±0.01	0.23±0.04
	^{35}Cl* $\mathbf{a}_0^{(1)}(\perp)$	−0.12	−0.26±0.17	
	$\mathrm{Re}[\mathbf{a}_1^{(1)}(\parallel,\perp)]$		0.43±0.10	0.69±0.17

much more reliable than commercial nominal zero-order waveplates. The results at 310 and 330 nm differ in the quarter-wave polarizing element used. A small percentage of linear polarization in our circularly polarized photolysis light would contribute to the isotropic (D_{iso}) signal, but not to the anisotropic (D_{aniso}) profile, effectively reducing the observed orientation moments. Frequent systematic checks were used to avoid errors caused by poor polarization (see Sec. II).

IV. DISCUSSION

The $\mathbf{a}_q^{(k)}(p)$ polarization moments of Rakitzis and Zare[10] carry information concerning the spatial distribution of angular momentum vectors. The polarization moments are equivalent to the spherical tensor moments that have been commonly used to describe the angular momentum distribution.[34] From the polarization moments, we obtain detailed information about the electronic dynamics that occur during the photodissociation process. The $\mathbf{a}_q^{(k)}(p)$ can be written in terms of the quantum dynamical functions $f_K(q,q')$ of Siebbeles *et al.*,[9]

$$\mathbf{a}_0^{(1)}(\perp)=\frac{f_1(1,1)}{f_0(1,1)}, \tag{3}$$

$$\mathbf{a}_1^{(1)}(\parallel,\perp)=\frac{-3\sqrt{2}f_1(1,0)}{f_0(0,0)+2f_0(1,1)}. \tag{4}$$

Equation (3) is written in the limit of a pure perpendicular transition, and would vanish for a pure parallel transition. The dynamical functions contain information on the dynamics of the photofragmentation process; in particular they depend on the molecular transition dipole (for a detailed discussion, we refer the reader elsewhere[9]). The dynamical treatment of Siebbeles *et al.* was formulated assuming adiabatic dissociation within the axial recoil approximation. A fully quantum treatment of photodissociation that relies only on the assumption of an electronic dipole transition in the molecule has recently been given by Mo *et al.*[18] However, following previous work on the photodissociation of Cl_2, we will assume that the axial recoil approximation is valid, and in the discussion that follows, we consider the effects of nonadiabatic transitions semiquantitatively in the adiabatic dissociation framework.[7]

If we consider a photofragmentation process producing two atomic fragments A and B, the dynamical functions can be related to the electronic dipole transition of the molecule AB, and are defined by[7]

$$f_K(q,q')=\sum_{m_{\mathrm{A}},m'_{\mathrm{A}}}(-1)^{j_{\mathrm{A}}+m_{\mathrm{A}}} \times\begin{pmatrix} j_{\mathrm{A}} & j_{\mathrm{A}} & K \\ -m_{\mathrm{A}} & m'_{\mathrm{A}} & q-q' \end{pmatrix} M_{j_{\mathrm{A}}\Omega_i m_{\mathrm{A}}}(M_{j_{\mathrm{A}}\Omega_i m'_{\mathrm{A}}})^*, \tag{5}$$

where j_{A} is the atomic A fragment angular momentum. The projection m_{A} along the recoil axis is quantized, and is directly equivalent to the familiar $(2j_{\mathrm{A}}+1)$ magnetic substates of angular momentum j_{A}.[34] The components of the initial (J_i) and final (J) electronic molecular angular momentum along the recoil axis are denoted Ω_i and Ω, respectively. The transition dipole matrix elements $M_{j_{\mathrm{A}}\Omega_i m_{\mathrm{A}}}$ can be calculated following the methods of Vasyutinskii and co-workers,[17] and require a knowledge of the matrix elements $T^{\Omega}_{j_{\mathrm{A}}m_{\mathrm{A}}j_{\mathrm{B}}m_{\mathrm{B}}}$ that correlate the excited molecular states Ω with the angular momentum states $|j,m_j\rangle$ of the atomic photofragments. Vasyutinskii and co-workers have evaluated T matrix elements using a first-order perturbation calculation in an atomic $|j,m_j\rangle$ basis by taking into account the long-range multipolar charge interaction of the atomic fragments.[38] For the two channels under consideration, the chlorine atoms have the same electronic parity and therefore the long-range interactions to be considered are quadrupole–quadrupole and dispersion (induced-dipole–induced-dipole) interactions.[39] The long-range effects of these interactions have been considered quantitatively for the molecular chlorine system by Saute *et al.*[40] As will be discussed later, by comparing the theoretically expected values of $\mathbf{a}_q^{(k)}(p)$ with the experimentally measured values, we can gain a detailed answer as to which states are involved in the photodissociation process. Such details provide the first step toward understanding which states may take part in the dissociation, and the mechanism for their interaction.

A. Cl($^2P_{3/2}$) atoms

According to the experimentally observed β parameter, ground-state Cl atoms at photolysis wavelengths of 310 and 330 nm are produced mostly via perpendicular transitions. Following Bracker *et al.*[7] we find that the two lowest states of 1_u symmetry correlate to atomic $|j_{\mathrm{A}},m_{\mathrm{A}}\rangle|j_{\mathrm{B}},m_{\mathrm{B}}\rangle$ states as

$$|1_u^{(1)}\rangle_A \xrightarrow{R\to\infty} \frac{1}{\sqrt{2}}\left(\left|\tfrac{3}{2}\tfrac{3}{2}\right\rangle\left|\tfrac{3}{2}-\tfrac{1}{2}\right\rangle+\left|\tfrac{3}{2}-\tfrac{1}{2}\right\rangle\left|\tfrac{3}{2}\tfrac{3}{2}\right\rangle\right), \tag{6}$$

$$|1_u^{(2)}\rangle_C \xrightarrow{R\to\infty} \left|\tfrac{3}{2}\tfrac{1}{2}\right\rangle\left|\tfrac{3}{2}\tfrac{1}{2}\right\rangle, \tag{7}$$

where R denotes the Cl_2 internuclear separation. To conveniently distinguish between the five states of 1_u symmetry,

Downloaded 24 Feb 2012 to 171.64.124.19. Redistribution subject to AIP license or copyright; see http://jcp.aip.org/about/rights_and_permissions

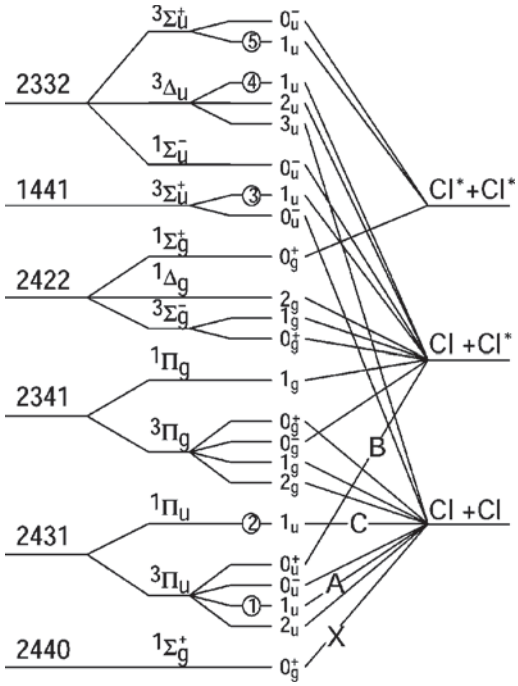

FIG. 4. Correlation diagram showing all of the electronic states of Cl_2, (Refs. 2 and 3). On the right-hand side ground-state $Cl(^2P_{3/2})$ and excited-state $Cl^*(^2P_{1/2})$ are denoted as Cl and Cl*, respectively, as in the text. The left-hand side shows the electronic configuration of the molecular orbitals $5\sigma_g 2\pi_u 2\pi_g^* 5\sigma_u^*$. The electronic terms are shown along with the projection of total electronic angular momentum, Ω. The five states of $\Omega=1_u$ symmetry that are important for the present discussion are labeled in energetic order from 1 to 5, as they are in the text, e.g., $1_u^{(1)}$ is the lowest state (*A* state). States *X*, *A*, *B*, and *C* are also highlighted for convenience.

we have labeled the ordering of the molecular $\Omega_u^{(n)}$ states as a superscript (n), see Fig. 4. The transition dipole (T) matrix elements show that the *C* state correlates to produce two $Cl(^2P_{3/2})$ atoms both with $m_j=+1/2$ [see Eq. (7)] and that the *A* state correlates to produce Cl atoms in a symmetric linear superposition of $m_j=+3/2$ and $m_j=-1/2$ [see Eq. (6)].

Previous measurements of the electronic alignment of the Cl atoms suggest that the *C* state is mostly responsible for the production of Cl atoms around 310 to 330 nm. Rakitzis *et al.*[6] measured an $\mathbf{a}_0^{(2)}(\perp)$ value of -0.50 ± 0.10, and an $\mathbf{a}_2^{(2)}(\perp)$ value of -0.32 ± 0.06, at a photolysis wavelength of 320 nm. We can convert the alignment parameters $(s_2,\alpha_2,\gamma_2,\eta_2)$ measured by Bracker *et al.*[7] at a photolysis wavelength of 355 nm, using

$$\tfrac{1}{5}(1+\beta)\mathbf{a}_0^2(\parallel)=s_2-2\alpha_2, \tag{8}$$

$$\frac{1}{5}\left(1-\frac{\beta}{2}\right)\mathbf{a}_0^2(\perp)=s_2+\alpha_2, \tag{9}$$

$$\mathbf{a}_1^2(\parallel,\perp)=-\frac{15}{\sqrt{6}}\gamma_2, \tag{10}$$

$$\frac{2}{3}\left(1-\frac{\beta}{2}\right)\mathbf{a}_2^2(\perp)=-\frac{5}{\sqrt{6}}\eta_2. \tag{11}$$

From the results of Bracker *et al.* we obtain $\mathbf{a}_0^{(2)}(\perp)=-0.35\pm0.04$ and $\mathbf{a}_2^{(2)}(\perp)=-0.15\pm0.04$. Following the method of calculating polarization moments from the transition diplole matrix elements as outlined previously, theory predicts that adiabatic dissociation via the *C* state produces a maximal $m_j=1/2$ alignment $\mathbf{a}_0^{(2)}(\perp)=-0.8$, and that the *A* state produces zero alignment $\mathbf{a}_0^{(2)}(\perp)=0$. Such results led Bracker *et al.* to the conclusion that homogeneous nonadiabatic transitions occur from the *C* to the *A* states, effectively reducing the observed $\mathbf{a}_0^{(2)}(\perp)$.[7]

From the theory, using Eq. (3), we calculate $\mathbf{a}_0^{(1)}(\perp)=0.258$ for dissociation via either the *A* or the *C* state, and the result is in excellent agreement with the measured $\mathbf{a}_0^{(1)}(\perp)$ value at 330 nm. The agreement between theory and experiment is not as good at 310 nm, although we have no *a priori* reason to believe that the measured results at 310 nm should differ significantly from the result obtained at 330 nm. In fact the theoretical result can be obtained by a simple calculation of the orientation of a $j=3/2$ atom in a magnetic substate $m_j=1/2$: $\mathbf{a}_0^{(1)}=m_j/\sqrt{j(j+1)}$.[34] Physically, we see that the single unit of angular momentum carried by the CP photon is shared equally between the two atoms: either two atoms both with $m_j=+1/2$, or both in a linear superposition of $m_j=+3/2$ and $-1/2$. In this case, measurement of the $\mathbf{a}_0^{(1)}(\perp)$ moment cannot distinguish between the 1_u states *A* or *C*. Calculating the third-order orientation moment $\mathbf{a}_0^{(3)}(\perp)$ for the above-mentioned states we find that when $m_j=+1/2$, $\mathbf{a}_0^{(3)}(\perp)=-0.31$, and a linear superposition of $m_j=+3/2$ and $-1/2$ yields $\mathbf{a}_0^{(3)}(\perp)=0.21$. To further understand the involvement of the $\mathbf{a}_0^{(3)}(\perp)$ moment in our data, we simulated profiles using values of $\mathbf{a}_0^{(1)}(\perp)$ and $\mathbf{a}_0^{(3)}(\perp)$ calculated previously, but fitting them with an $\mathbf{a}_0^{(1)}(\perp)$ only. It was found that the $\mathbf{a}_0^{(3)}(\perp)$ modified the fitted $\mathbf{a}_0^{(1)}(\perp)$ by up to 20%. For the case of $m_j=+1/2$, the fitted $\mathbf{a}_0^{(1)}(\perp)$ may be underestimated by up to 20%, which may account for the difference in the fitted and integrated values shown in Table I. However, the $\mathbf{a}_0^{(1)}(\perp)$ orientation moment cannot distinguish between the *A* and the *C* states. Combined with the results for $\mathbf{a}_0^{(2)}(\perp)$, we conclude that the dominant channel for producing Cl+Cl is adiabatic dissociation via the *C* state with contributions from nonadiabatic transitions between the *C* state and the *A* state.

B. Cl*($^2P_{1/2}$) atoms

Previous studies of the ultraviolet photodissociation of molecular chlorine indicate that excited-state Cl* atoms are produced by dissociation via mixed (parallel and perpendicular) transitions in the region of 270–400 nm.[3] Evidence for the mixed transitions include the nonlimiting β parameter,[5] and the measurement of the $\mathrm{Im}[\mathbf{a}_1^{(1)}(\parallel,\perp)]$ orientation moment that depends on the coherence between the dissociation via parallel and perpendicular transitions.[8] In previous work, we observed an oscillation in the $\mathrm{Im}[\mathbf{a}_1^{(1)}(\parallel,\perp)]$ as a function of photolysis wavelength. This oscillation results from the photolysis energy dependence of the coherence between parallel and perpendicular transitions. At the photolysis wavelength 330 nm, the number of Cl* atoms produced via parallel and perpendicular transitions is approximately equal.

Downloaded 24 Feb 2012 to 171.64.124.19. Redistribution subject to AIP license or copyright; see http://jcp.aip.org/about/rights_and_permissions

The magnitude of the coherent $\mathbf{a}_1^{(1)}(\parallel,\perp)$ moment can be largest when there are equal contributions from parallel and perpendicular states, assuming that the transitions are perfectly in phase with each other. Taking the imaginary and real parts of the $\mathbf{a}_1^{(1)}(\parallel,\perp)$, as mentioned in Sec. III, the $\mathrm{Im}[\mathbf{a}_1^{(1)}(\parallel,\perp)]$ and $\mathrm{Re}[\mathbf{a}_1^{(1)}(\parallel,\perp)]$ are 90° out of phase and the measured $\mathrm{Im}[\mathbf{a}_1^{(1)}(\parallel,\perp)]$ at 330 nm is small (0.032 ± 0.005), despite the fact that the contributions from parallel and perpendicular transitions are almost equal at this photolysis wavelength. Consequently, we might expect the $\mathrm{Re}[\mathbf{a}_1^{(1)}(\parallel,\perp)]$ to be large. This supposition is supported by the oscillation in $\mathrm{Im}[\mathbf{a}_1^{(1)}(\parallel,\perp)]$ as a function of photolysis wavelength that was observed by Kim *et al.*: The oscillation appears to change sign at around 330 nm.[8] The maximum allowed value of the $\mathrm{Re}[\mathbf{a}_1^{(1)}(\parallel,\perp)]$ can be calculated by rotating a maximal $\mathbf{a}_0^{(1)}(\perp)$ distribution using Wigner rotation matrices.[34]

$$\begin{aligned}\mathrm{Re}[\mathbf{a}_1^{(1)}] &= \tfrac{1}{2}(\mathbf{a}_{+1}^{(1)} - \mathbf{a}_{-1}^{(1)}) \\ &= \tfrac{1}{2}\mathbf{a}_0^{(1)}[d_{+10}^{(1)}(\theta) - d_{-10}^{(1)}(\theta)] \\ &= \frac{1}{\sqrt{2}}\mathbf{a}_0^{(1)} \sin\theta. \end{aligned} \tag{12}$$

The $d_{q',q}^{k}(\theta)$ are the real rotation matrices, and $\theta = 90°$. For $j = 1/2$ the maximum $\mathbf{a}_0^{(1)}(\perp)$ is 0.577, and the maximum calculated $\mathrm{Re}[\mathbf{a}_1^{(1)}(\parallel,\perp)]$ is 0.408, which agrees with the value that we have measured (0.43 ± 0.10).

From the present study the most striking effect that we observe is a negative orientation for the Cl* atom, i.e., the Cl* fragments are oriented with the opposite sense compared to the photolysis laser CP light. We may calculate the expected $\mathbf{a}_0^{(1)}(\perp)$ from the electronic correlation diagram using the T matrix in the same manner as described previously. In previous work, we suggested that the production of Cl* atoms occurs by direct absorption via a parallel transition to the $B\,0_u^+$ state, and also by absorption via a perpendicular transition to the $C\,1_u^{(2)}$ state followed by some nonadiabatic transition. The nonadiabatic transition may involve either an inhomogeneous Coriolis mechanism coupling from the C to the B state, or a homogeneous radial derivative coupling (RDC) to a higher state of 1_u symmetry;[39] see Fig. 5. We exclude direct dissociation via one of the higher 1_u states by the Franck–Condon principle, noting the large cross section for production of Cl atoms from the C state. The states that correlate to produce Cl* fragments that we will consider are two states of 1_u symmetry ($^3\Delta_u$ and $^3\Sigma_u^+$) and one state of 0_u^+ symmetry (the $B\,^3\Pi_u$ state). For these states the correlations in terms of atomic fragments are[40]

$$|0_u^+\rangle_B \xrightarrow{R\to\infty} \tfrac{1}{2}(|\tfrac{3}{2}\tfrac{1}{2}\rangle|\tfrac{1}{2}-\tfrac{1}{2}\rangle - |\tfrac{1}{2}-\tfrac{1}{2}\rangle|\tfrac{3}{2}\tfrac{1}{2}\rangle - |\tfrac{3}{2}-\tfrac{1}{2}\rangle|\tfrac{1}{2}\tfrac{1}{2}\rangle + |\tfrac{1}{2}\tfrac{1}{2}\rangle|\tfrac{3}{2}-\tfrac{1}{2}\rangle), \tag{13}$$

$$|1_u^{(3)}\rangle_\Sigma \xrightarrow{R\to\infty} \frac{1}{\sqrt{2}}(|\tfrac{3}{2}\tfrac{3}{2}\rangle|\tfrac{1}{2}-\tfrac{1}{2}\rangle + |\tfrac{1}{2}-\tfrac{1}{2}\rangle|\tfrac{3}{2}\tfrac{3}{2}\rangle), \tag{14}$$

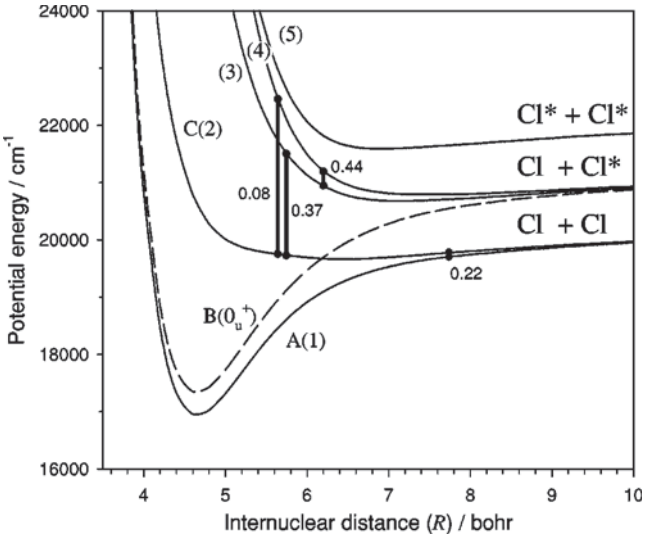

FIG. 5. *Ab initio* potential energy curves as a function of the internuclear separation R, showing the excited states of Cl_2 relevant to the present discussion. Solid curves are the states of 1_u symmetry, labeled as in Fig. 4, the dashed curve is the B state. The axes have been scaled to highlight the potential energy curves shown, and the ground electronic state of Cl_2 has been omitted for convenience. The peak positions of *ab initio* calculated radial derivative coupling matrix elements $g_{ij} = \langle 1_u^{(i)}|(\partial/\partial R)1_u^{(j)}\rangle$ are shown as solid vertical bars between the 1_u states. The magnitudes of these coupling terms are also shown in units of bohr^{-1}.

$$|1_u^{(4)}\rangle_\Delta \xrightarrow{R\to\infty} \frac{1}{\sqrt{2}}(|\tfrac{3}{2}\tfrac{1}{2}\rangle|\tfrac{1}{2}\tfrac{1}{2}\rangle + |\tfrac{1}{2}\tfrac{1}{2}\rangle|\tfrac{3}{2}\tfrac{1}{2}\rangle). \tag{15}$$

Using these correlations and Eqs. (3)–(5) as before, we find that the B state would produce zero orientation $\mathbf{a}_0^{(1)}(\perp)$ for either the Cl or the Cl* photofragments: the initial $\Omega = 0$ leaves no projection for the final atomic fragments. The $1_u^{(3)}$ and the $1_u^{(4)}$ states would produce maximal Cl* orientations but of opposite sign, $\mathbf{a}_0^{(1)}(\perp) = -0.577$ for the $1_u^{(3)}$ state and $\mathbf{a}_0^{(1)}(\perp) = +0.577$ for the $1_u^{(4)}$ state. We immediately assign the major portion of the observed Cl* fragments to dissociation via the $1_u^{(3)}$ state because of the observed negative orientation in the lab frame. At a photolysis wavelength of 310 nm, the spatial distribution of the fragments $\beta(\mathrm{Cl}^*) = 0.32$,[5] which implies that 88% of the Cl* fragments originate from a perpendicular transition. If all of these fragments dissociated via RDC to the $1_u^{(3)}$ state, we might expect to see an $\mathbf{a}_0^{(1)}(\perp)$ value of $0.88 \times (-0.577) = -0.51$. The 12% that originate from the parallel (B state) transition have zero orientation and reduce the observed orientation from the maximal value. The observed $\mathbf{a}_0^{(1)}(\perp)$ for ^{35}Cl* at these energies (-0.27 ± 0.06) is much smaller than maximal, but suggests that at least $47 \pm 10\%$ of the ^{35}Cl* dissociate via RDC to the $1_u^{(3)}$ state with the remaining percentage having a net zero orientation: We shall discuss possible mechanisms in the following. For ^{37}Cl*, the estimate of percentage dissociation via RDC to the $1_u^{(3)}$ state is $52 \pm 12\%$: We have no reason to believe that the different isotopes of Cl would produce significantly different results. At 330 nm $\beta(\mathrm{Cl}^*) = -0.12$,[5] implying 59% of the Cl* atoms originate from a perpendicular transition. If all of the fragments originating from a perpendicular transition were to dissociate via the $1_u^{(3)}$ state we

Downloaded 24 Feb 2012 to 171.64.124.19. Redistribution subject to AIP license or copyright; see http://jcp.aip.org/about/rights_and_permissions

TABLE II. *Ab initio* relative absorption coefficients from the ground (X) to the first three excited states of Cl_2 are shown at wavelengths of 310 and 330 nm. The nonadiabatic transition probability from the C to the $1_u^{(3)}$ state, P^{RZD}, was calculated using the semiclassical expression of Rosen–Zener–Demkov (Refs. 39 and 42), where the parameters were fitted only from the adiabatic energies. The calculations yield an estimated β parameter for Cl* photofragments that is in very good agreement with experimental results of Samartzis *et al.* (Ref. 5).

	310 nm	330 nm
$A-X$ absorption	3.160×10^{-5}	1.261×10^{-4}
$B-X$ absorption	3.277×10^{-4}	1.392×10^{-3}
$C-X$ absorption	0.2908	0.4461
$P^{RZD}C-1_u^{(3)}$	5.42×10^{-3}	3.52×10^{-3}
β(Cl*) *ab initio*	0.25	−0.21
β(Cl*)[a]	0.32	−0.12

[a]Reference 5.

would expect $\mathbf{a}_0^{(1)}(\perp)=-0.34$. From our measured value of $\mathbf{a}_0^{(1)}(\perp)(-0.26\pm0.17)$ we estimate that at least $52\pm44\%$ of all $^{35}Cl^*$ fragments dissociate via the $1_u^{(3)}$ state.

As mentioned previously, some remaining percentage of the Cl* fragments that originate from a perpendicular transition must have net zero orientation, and this may occur by absorption to the C state followed by:

(a) transition by Coriolis mechanism to the B state, with $\Omega=0$,
(b) transition by RDC mechanism equally to the $1_u^{(3)}$ and $1_u^{(4)}$ states producing fragments with opposite orientation that cancel to give net zero orientation.

Coriolis coupling will be dependent on the rotational temperature of the chlorine gas, and this temperature has not been fully characterized for our pulsed expansion. It may be possible to investigate the Coriolis mechanism by selective excitation of Cl_2 molecular rotational states, or by altering the temperature or collision conditions of the expansion in a controlled manner. However, for the present experiments, we believe that these effects are small.[3] *Ab initio* calculations predict a negligibly small Coriolis transition probability (on the order of 10^{-6}) for rotational temperatures of 100 to 300 K.[12]

From the above-mentioned arguments, we discount mechanism (a). Taking stock of the approximations implied by the theoretical treatment, it can be seen that our estimates of the RDC transition to the $1_u^{(3)}$ state are conservative. Recall that some of the fragments have orientation of opposite sense, as in condition (b) noted previously. Estimates of relative absorption coefficients, β parameters, and nonadiabatic transition probabilities from the C to the $1_u^{(3)}$ state calculated in our previous *ab initio* study[11] are shown in Table II. For the present study, the *ab initio* spin–orbit configuration-interaction (CI) calculations of the potential energy curves of Cl_2 have been extended to include calculation of the RDC matrix elements, $g_{ij}=\langle\Psi^{(i)}|(\partial/\partial R)\Psi^{(j)}\rangle$, between the different adiabatic states of 1_u symmetry. The theoretical methods are similar to those previously applied to ICl molecule.[41] In the calculations of RDC elements, we have neglected the so-called molecular orbital derivative terms, whose contributions are usually small. This simplification is partly justified because the molecular orbitals do not change very much at the longer bond distances of interest.

As typical models of the RDC mechanism, curve crossing Landau–Zener and noncrossing Rosen–Zener–Demkov (RZD) models are well known.[39,42] In the latter model, the energy difference between the two diabatic states $\Delta=H_{ii}-H_{jj}$ is constant and the diabatic coupling element H_{ij} depends on the internuclear distance R as $H_{ij}=A\exp(-\alpha R)$. Inspecting the potential curves and the corresponding adiabatic CI wave functions, the nonadiabatic behavior of the 1_u states was found to follow the RZD model approximately. For each pair of coupled adiabatic states $\Psi^{(i)}$ and $\Psi^{(j)}$, the matrix element g_{ij} behaves as

$$g_{ij}=\frac{\alpha}{4}\frac{1}{\cosh\{\alpha(R-R_{max})\}}, \tag{16}$$

with a peak value of $\alpha/4$ at $R=R_{max}$, where $A\times\exp(-\alpha R_{max})=\Delta/2$ is satisfied. We have fitted the parameters α, A, Δ, R_{max} from the *ab initio* results. The Δ values were determined from the adiabatic energy difference at R_{max}, divided by $\sqrt{2}$: This relation must be satisfied for the noncrossing-type RZD model. R_{max} and the peak values of some of the coupling elements are indicated schematically in Fig. 5, e.g., g_{23} peaks at $R_{max}=5.7$ bohr (1 bohr $=5.29\times10^{-11}$ m). The fitted parameters were used to compute RZD nonadiabatic transition probabilities,[39,42]

$$P^{RZD}=\frac{1}{1+\exp\left(\frac{\pi\Delta}{\hbar\alpha v}\right)}, \tag{17}$$

where v is the relative velocity of the fragment atoms at R_{max}. It follows from Eq. (17) that as v becomes large, or Δ becomes small, P^{RZD} approaches the diabatic limiting value of 1/2. We therefore expect that $P_{2\to1}^{RZD}$ and $P_{3\to4}^{RZD}$ can be quite large since the coupling states correlate to common dissociation limits, as Fig. 5 shows, and Δ is very small for both couplings. On the other hand, $P_{2\to3}^{RZD}$ and $P_{2\to4}^{RZD}$ are expected to be rather small since the magnitude of Δ corresponds to the spin–orbit splitting of the Cl atom.

From their alignment experiments at a photolysis wavelength of 355 nm (see Sec. IV B) Bracker *et al.*[7] estimated a strong nonadiabatic transition probability of $P_{2\to1}=0.60\pm0.04$ from the C to A state. From our alignment measurements[6] at 320 nm we estimate $P_{2\to1}=0.38\pm0.13$. The A and C states converge adiabatically to the same atomic limit, and the RDC matrix element g_{21} has a peak at a longer distance ($R_{max}=7.7$ bohr), making the transition nearly resonant, thus, it is no surprise that the transition probability is large. At the photolysis wavelength 355 nm, Eq. (17) gives $P_{2\to1}^{RZD}=0.41$, in reasonable agreement with the large transition probability observed, and at 320 nm we estimate $P_{2\to1}^{RZD}=0.42$, which is in excellent agreement with our experiments.

For the present calculations, we obtained fairly large near-resonant nonadiabatic transition probabilities of $P_{3\to4}^{RZD}=0.273(0.256)$, and small noncrossing-type nonadiabatic

Downloaded 24 Feb 2012 to 171.64.124.19. Redistribution subject to AIP license or copyright; see http://jcp.aip.org/about/rights_and_permissions

transition probabilities of $P_{2\to3}^{\mathrm{RZD}}=1.67\times10^{-3}(0.952\times10^{-3})$ and $P_{2\to4}^{\mathrm{RZD}}=4.5\times10^{-20}(7.9\times10^{-22})$ for $\lambda=310$ (330) nm respectively. The $P_{2\to3}^{\mathrm{RZD}}$ are a little smaller than our previous theoretical estimates (shown in Table II), which were calculated using only the adiabatic energy differences without the RDC elements.[11] Part of the underestimation comes from our approximate evaluation of the RDC elements, especially for those with peaks at shorter bond distances, where the variation of the molecular orbitals cannot be neglected. In spite of this uncertainty, we believe that the one-step nonadiabatic transition from the *C* state to the $1_u^{(4)}$ state is negligible. Furthermore, Cl* dissociation on the $1_u^{(4)}$ state should originate from the *C* state via the intermediate $1_u^{(3)}$ state by two-step transition, since $P_{2\to4}^{\mathrm{RZD}}\ll P_{2\to3}^{\mathrm{RZD}}\times P_{3\to4}^{\mathrm{RZD}}$.

Reviewing the data available, we make the following hypotheses. After initial absorption to the *C* state, less than 1% of chlorine molecules make a nonadiabatic transition to the $1_u^{(3)}$ state. The majority of the fragments go on to produce two ground state Cl atoms adiabatically via the *C* state, or by nonadiabatic crossing to the *A* state. By measuring the Cl* fragments, however, we are really selecting a special subset of molecules that absorb the ultraviolet light: Therefore, the absolute transition probability from the *C* state to the $1_u^{(3)}$ state need not be large. In order to produce the observed mixed β parameter, the number of molecules that experience a nonadiabatic transition should be of the same order as the number that are directly absorbed to the *B* state: see Table II. However, after transition to the $1_u^{(3)}$ state, molecules may experience a strong nonadiabatic transition to the $1_u^{(4)}$ state, as a result of the fairly large near-resonant nonadiabatic transition probability $P_{3\to4}^{\mathrm{RZD}}$ (cf., the strong transition between the *C* and *A* states estimated by Bracker *et al.*[7]). This behavior would explain the reduced from maximal values of the orientation parameter that we have measured for Cl* atoms.

Consider the particular case of ^{35}Cl* at 310 nm (see prior text). We return to the question of the partitioning of the fragment atoms between the different states of 1_u symmetry. Recall that we attributed the observed negative $\mathbf{a}_0^{(1)}(\perp)$ to 12% dissociating via parallel transition to the **B** state, with zero orientation, and $47\pm10\%$ dissociating via the $1_u^{(3)}$ state with maximal orientation $\mathbf{a}_0^{(1)}(\perp)=-0.577$. The remaining percentage of fragments originates from a perpendicular transition ($41\pm10\%$). We split this percentage equally between the $1_u^{(3)}$ and $1_u^{(4)}$ states, with equal and opposite orientations that cancel to give a net zero orientation, From this data we estimate a transition probability from the $1_u^{(3)}$ to the $1_u^{(4)}$ state of $P_{3\to4}=0.23\pm0.06$. This estimate is in excellent agreement with the theoretically calculated RZD nonadiabatic transition probability $P_{3\to4}^{\mathrm{RZD}}=0.27$. In total, the $\mathbf{a}_0^{(1)}(\perp)$ measurements suggest that $67\pm16\%$ of ^{35}Cl* atoms dissociate via the $1_u^{(3)}(^3\Sigma_{1u}^+)$ state, and $21\pm6\%$ dissociate via the $1_u^{(4)}(^3\Delta_{1u})$ state. Thus, we conclude that dissociation via the $1_u^{(3)}(^3\Sigma_{1u}^+)$ state plays the major role in the production of Cl* atoms.

V. CONCLUSIONS

Molecular chlorine was photodissociated at 310 and 330 nm using circularly polarized light. Orientation moments of the electronic angular momentum of product ground-state $\mathrm{Cl}(^2P_{3/2})$ and excited-state $\mathrm{Cl}^*(^2P_{1/2})$ chlorine atoms were measured, and the contributions from both coherent and incoherent dissociation mechanisms were resolved. The experimental results for Cl* can be explained by nonadiabatic transitions from the $C\,^1\Pi_{1u}$ state to higher states of 1_u symmetry, induced by noncrossing-type radial derivative coupling. *Ab initio* calculations indicate significant Rosen–Zener–Demkov type radial derivative couplings between the $1_u^{(2)}(C\,^1\Pi_{1u})$ and $1_u^{(3)}(^3\Sigma_{1u}^+)$ states, and between the $1_u^{(3)}(^3\Sigma_{1u}^+)$ and $1_u^{(4)}(^3\Delta_{1u})$ states. At the photolysis wavelength of 310 nm, 88% of the observed Cl* fragments originate from a perpendicular transition. The orientation measurements suggest that $67\pm16\%$ of ^{35}Cl* atoms dissociate via the $1_u^{(3)}(^3\Sigma_{1u}^+)$ state, and $21\pm6\%$ dissociate via the $1_u^{(4)}(^3\Delta_u)$ state. We conclude that nonadiabatic transitions induced by noncrossing-type radial derivative coupling play a dominant role in controlling the orientation of the resulting Cl* atom photofragments.

The results demonstrate that measurements of the electronic orientation not only provide a detailed picture of the electronic states accessed but also of the nonadiabatic transitions that occur far from the Franck–Condon region. Taken together, the present measurements of photofragment orientation caused by photolysis with circularly polarized light, the previous measurements of photofragment orientation[8] and alignment[6,7] caused by photolysis with linearly polarized light, provide new information on how simple molecules separate into their constituent atoms under the action of radiation.

ACKNOWLEDGMENTS

We are grateful to Oleg Vasyutinskii and David van Baak for useful discussions. S.Y. thanks Hiroki Nakamura at IMS, Okazaki, for useful discussions. Z.H.K. gratefully acknowledges receipt of a Dr. Franklin Veatch Memorial Fellowship. This work was funded by the National Science Foundation under Grant No. CHE-99-00305. S.Y. was supported by a Grants-in-Aid for Scientific Research from the Ministry of Education, Science, Culture, and Sports of Japan, and by Research and Development Applying Advanced Computational Science and Technology, Japan Science and Technology Corporation.

[1] G. Herzberg, *Molecular Spectra and Molecular Structure. I. Spectra of Diatomic Molecules* (van Nostrand Reinhold, New York, 1950).
[2] R. S. Mulliken, Phys. Rev. **36**, 1440 (1930).
[3] Y. Matsumi, K. Tonokura, and M. Kawasaki, J. Chem. Phys. **97**, 1065 (1992).
[4] P. C. Samartzis, I. Sakellariou, T. Gougousi, and T. N. Kitsopoulos, J. Chem. Phys. **107**, 43 (1997).
[5] P. C. Samartzis, B. L. Bakker, T. P. Rakitzis, D. H. Parker, and T. N. Kitsopoulos, J. Chem. Phys. **110**, 5201 (1999).
[6] T. P. Rakitzis, S. A. Kandel, A. J. Alexander, Z. H. Kim, and R. N. Zare, J. Chem. Phys. **110**, 3351 (1999).
[7] A. S. Bracker, E. R. Wouters, A. G. Suits, and O. S. Vasyutinskii, J. Chem. Phys. **110**, 6749 (1999).
[8] Z. H. Kim, A. J. Alexander, S. A. Kandel, T. P. Rakitzis, and R. N. Zare, Faraday Discuss. **113**, 27 (1999).
[9] L. Siebbeles, M. Glass-Maujean, O. S. Vasyutinskii, J. A. Beswick, and O. Roncero, J. Chem. Phys. **100**, 3610 (1994).

Downloaded 24 Feb 2012 to 171.64.124.19. Redistribution subject to AIP license or copyright; see http://jcp.aip.org/about/rights_and_permissions

[10] T. P. Rakitzis and R. N. Zare, J. Chem. Phys. **110**, 3341 (1999).
[11] A. J. Alexander, R. N. Zare, Z. H. Kim, and S. Yabushita, Faraday Discuss. **113**, 83 (1999).
[12] Y. Asano and S. Yabushita (unpublished).
[13] R. J. v. Brunt and R. N. Zare, J. Chem. Phys. **48**, 4304 (1968).
[14] O. S. Vasyutinskii, JETP Lett. **31**, 428 (1980).
[15] O. S. Vasyutinskii, Sov. Phys. JETP **54**, 855 (1981).
[16] E. W. Rothe, U. Krause, and R. Duren, Chem. Phys. Lett. **72**, 100 (1980).
[17] D. V. Kupriyanov and O. S. Vasyutinskii, Chem. Phys. **171**, 25 (1993).
[18] Y. Mo and T. Suzuki, J. Chem. Phys. **112**, 3463 (2000).
[19] L. D. A. Siebbeles and J. A. Beswick, J. Chem. Soc., Faraday Trans. **88**, 2565 (1992).
[20] A. J. Alexander and R. N. Zare, Acc. Chem. Res. **33**, 199 (2000).
[21] Z. H. Kim, A. J. Alexander, and R. N. Zare, J. Phys. Chem. A **103**, 10144 (2000).
[22] R. N. Zare, Faraday Discuss. Chem. Soc. **84**, 180 (1987).
[23] E. Hasselbrink, J. R. Waldeck, and R. N. Zare, Chem. Phys. **126**, 191 (1988).
[24] D. V. Kupriyanov, B. N. Sevastianov, and O. S. Vasyutinskii, Z. Phys. D: At., Mol. Clusters **15**, 105 (1990).
[25] A. G. Evseev, D. V. Kupriyanov, B. V. Picheyev, B. N. Sevastianov, and O. S. Vasyutinskii, Chem. Phys. **171**, 45 (1993).
[26] D. V. Kupriyanov, B. V. Picheyev, and O. S. Vasyutinskii, J. Phys. B **26**, L803 (1993).
[27] B. V. Picheyev, A. G. Smolin, and O. S. Vasyutinskii, J. Phys. Chem. **101**, 7614 (1997).
[28] K. O. Korovin, B. V. Picheyev, O. S. Vasyutinskii, H. Valipour, and D. Zimmerman, J. Chem. Phys. **112**, 2059 (2000).
[29] W. R. Simpson, A. J. Orr-Ewing, S. A. Kandel, T. P. Rakitzis, and R. N. Zare, J. Chem. Phys. **103**, 7299 (1995).
[30] M. Born and E. Wolf, *Principles of Optics*, 2nd ed. (Macmillan, New York, 1964).
[31] J. D. Jackson, *Classical Electrodynamics*, 2nd ed. (Wiley, New York, 1975).
[32] Y. Mo and T. Suzuki, J. Chem. Phys. **109**, 4691 (1998).
[33] T. P. Rakitzis, S. A. Kandel, and R. N. Zare, J. Chem. Phys. **107**, 9382 (1997).
[34] R. N. Zare, *Angular Momentum: Understanding Spatial Aspects in Chemistry and Physics* (Wiley, New York, 1988).
[35] T. P. Rakitzis, S. A. Kandel, and R. N. Zare, J. Chem. Phys. **107**, 9382 (1997).
[36] Note that all β parameters quoted in the present paper are modified for photolysis with circular polarized light.
[37] R. N. Zare, Faraday Discuss. **113**, 79 (1999).
[38] J. A. Beswick and O. S. Vasyutinskii, Comments At. Mol. Phys. **34**, 69 (1998).
[39] E. E. Nikitin and S. Umanskii, *Theory of Slow Atomic Collisions* (Springer, New York, 1984).
[40] M. Saute, B. Bussery, and M. Aubert-Frécon, Mol. Phys. **51**, 1459 (1984).
[41] S. Yabushita, J. Mol. Struct.: THEOCHEM **461-462**, 523 (1999).
[42] H. Nakamura, in *Dynamics of Molecules and Chemical Reactions*, edited by R. E. Wyatt and J. Z. H. Zhang (Marcel Dekker, New York, 1996).

Downloaded 24 Feb 2012 to 171.64.124.19. Redistribution subject to AIP license or copyright; see http://jcp.aip.org/about/rights_and_permissions